

# Fourth level MSSM inflation from new flat directions

Sayantana Choudhury<sup>1</sup> and Supratik Pal<sup>1,2</sup>

<sup>1</sup>*Physics and Applied Mathematics Unit, Indian Statistical Institute, 203 B.T. Road, Kolkata 700 108, India*

<sup>2</sup>*Bethe Center for Theoretical Physics and Physikalisches Institut der Universität Bonn, Nussallee 12, 53115 Bonn, Germany*

We propose a model of inflation driven by minimal extension of SUSY, commonly known as MSSM. Starting from gauge invariant flat directions in the  $n = 4$  level comprising of **QQQL**, **QuQd**, **QuLe** and **uude**, we construct the inflaton potential and employ it to investigate for its consequences around the saddle point arising from the non-vanishing fourth derivative of the original potential. To this end, we derive the expressions for the important parameters in MSSM inflation using the loop corrected potential. We further estimate the observable parameters and find them to fit well with recent observational data from WMAP7 by using the code CAMB. We also explore the possibility of primordial black hole formation from our model. Finally, we analyze one loop RGE and compute different phenomenological parameters which could be precisely determined in LHC or future Linear Colliders.

## I. INTRODUCTION

The paradigm of primordial inflation is, by far, the most satisfactory explanation for early universe phenomena [1]. As a general prescription, inflation occurs due to a slowly rolling scalar field, the inflaton, dynamically giving rise to an epoch of accelerated expansion dominated by a false vacuum [2]. Primordial quantum fluctuations of inflaton are responsible for creation of matter content and observed perturbations in the Cosmic Microwave Background Radiation (CMBR). Further, slow-roll inflationary scenario generically predicts almost Gaussian adiabatic perturbations with a nearly flat spectrum, which conforms well with the latest observations.

Recently, some interesting proposition of inflationary model building was brought forth by Minimally Supersymmetric Standard Model (MSSM) where the inflaton is a gauge invariant [3, 4]  $n = 4$  level combination of scalar superpartners squark and slepton fields and fermionic superpartner gauginos which are candidate Cold Dark Matter (CDM) particles. However the original potential for  $n = 4$  level is unable to extract a suitable symmetry along the flat direction. To serve this purpose the usual way is to incorporate *saddle point mechanism* to the MSSM potential leading to vanishing of the second derivative and the slow roll phase is driven by the next leading order derivative of the potential [1, 3–6]. In most of the phenomenological situations, a fine tuning mechanism is needed to place the flat direction field to the immediate neighborhood of the *saddle point*. It is worthwhile to mention that MSSM inflation occurs at a comparative lower scale. This is in strong contrast with the conventional class of models where the unfamiliar inflaton couplings to Standard Model (SM) are originated through arbitrary gauge singlets leading to the field magnitudes at GUT scale or higher, and hence, face problems in satisfactory quantitative estimation of a huge sector of the post-inflationary evolution i.e. thermal history of the early Universe, baryon asymmetry and CDM. Herein lies the most appealing feature of MSSM inflation for which known SM couplings are measurable in laboratory experiments such as Large Hadron Collider (LHC) [7] or future

linear colliders.

In the present article we will consider a specific MSSM scenario where, for a specific choice of soft supersymmetry (SUSY) breaking parameters  $A$  (trilinear couplings) and the inflaton mass  $m_\phi$ , the potential is D-flat along the **QQQL**, **QuQd**, **QuLe** and **uude** directions. For our model existence of *saddle point* is guaranteed by the non-vanishing fourth derivative of the potential, which makes the potential more flat than the previous ones. This implies more precise information in the RG flow. As we will show, this is the highest level of precision constraint one can impose on RG flow keeping the effective potential renormalizable in the vicinity of the *saddle point*. Our primary intention is to investigate for the analytical as well as the numerical expressions for different observational parameters for MSSM inflation with these new flat directions. As it will turn out, they match quite well with latest observational data from WMAP7 [8] and are expected to fit well with upcoming data from PLANCK [9]. Additionally we have explicitly shown the connection between running and running of the running of spectral index to the Primordial Black Hole (PBH) formation. To this end we get the fine tuned parameter space which is also in good agreement with present estimates of cosmological frameworks. We have further explored features of the MSSM from the solution of one loop RGE which could be measured by LHC or future linear collider.

## II. FLAT DIRECTIONS AND POTENTIAL AROUND SADDLE POINT

Let us start with  $n = 4$  level superpotential [19]

$$W_4^{nr} = \frac{1}{M} \left[ \sum_{I=1}^{24} \alpha_I (\mathbf{QQQL})_I + \sum_{I=1}^{81} \beta_I (\mathbf{QuQd})_I + \sum_{I=1}^{81} \gamma_I (\mathbf{QuLe})_I + \sum_{I=1}^{27} \delta_I (\mathbf{uude})_I \right]; \quad (1)$$

The renormalizable flat directions of the MSSM at  $n=4$  level correspond to the gauge invariant monomials subject to the four additional complex constraints [19] two

each from

$$F_{H_u}^\alpha = \mu H_d^\alpha + \lambda_U^{ab} Q_a^\alpha u_b = 0, \quad (2)$$

$$F_{H_d}^\alpha = -\mu H_u^\alpha + \lambda_D^{ab} Q_a^\alpha d_b + \lambda_E^{ab} L_a^\alpha e_b = 0, \quad (3)$$

which can lift the flat directions which do not contain a Higgs field. Here  $\lambda_U, \lambda_D$  and  $\lambda_E$  are the Yukawa couplings,  $H_u, H_d$  are the Higgs superfield and the  $\mu$ - term appears in the renormalizable part of the superpotential of MSSM. Consequently the equation(1) breaks into four parts, each one of them now being flat:

$$W_4^{(1)} = \frac{1}{M} \sum_{I=1}^{24} \alpha_I (\mathbf{Q}\mathbf{Q}\mathbf{Q}\mathbf{L})_I, \quad (4)$$

$$W_4^{(2)} = \frac{1}{M} \sum_{I=1}^{81} \beta_I (\mathbf{Q}\mathbf{u}\mathbf{Q}\mathbf{d})_I, \quad (5)$$

$$W_4^{(3)} = \frac{1}{M} \sum_{I=1}^{81} \gamma_I (\mathbf{Q}\mathbf{u}\mathbf{L}\mathbf{e})_I, \quad (6)$$

$$W_4^{(4)} = \frac{1}{M} \sum_{I=1}^{27} \delta_I (\mathbf{u}\mathbf{u}\mathbf{d}\mathbf{e})_I, \quad (7)$$

resulting in  $W_4^{(i)} \approx \frac{\lambda_i}{4M} \Phi^4 \forall i (= 1, 2, 3, 4)$ . Considering any one of the above flat directions leads to the one loop corrected effective potential

$$V(\phi, \theta) = \frac{1}{2} m_\phi^2 \phi^2 + \frac{\lambda_4 A}{4M} \phi^4 \text{Cos}(4\theta + \theta_A) + \frac{\lambda_4^2}{M^2} \phi^6, \quad (8)$$

for all  $i$ . Here we define  $\lambda_4 = \lambda_{4,0} \left[ 1 + D_3 \log \left( \frac{\phi^2}{\mu_0^2} \right) \right]$ ,  $A = \frac{A_0 \left[ 1 + D_2 \log \left( \frac{\phi^2}{\mu_0^2} \right) \right]}{\left[ 1 + D_3 \log \left( \frac{\phi^2}{\mu_0^2} \right) \right]}$  and  $m_\phi^2 = m_0^2 \left[ 1 + D_1 \log \left( \frac{\phi^2}{\mu_0^2} \right) \right]$  and in  $\mathbf{G}_{\text{MSSM}} = \mathbf{SU}(3)_C \otimes \mathbf{SU}(2)_L \otimes \mathbf{U}(1)_Y$  the representative flat direction field content is given by

$$\begin{aligned} \mathbf{Q}_a^{\mathbf{I}_1} &= \frac{1}{\sqrt{2}} (\Phi, 0)^T, \mathbf{Q}_b^{\mathbf{I}_2} = \frac{1}{\sqrt{2}} (\Phi, 0)^T, \mathbf{Q}_c^{\mathbf{I}_3} = \frac{1}{\sqrt{2}} (\Phi, 0)^T, \\ \mathbf{L}_3^{\mathbf{I}_4} &= \frac{1}{\sqrt{2}} P_d(0, \Phi)^T, \mathbf{d}_a^{\mathbf{B}_1} = \frac{\Phi}{\sqrt{2}}, \mathbf{u}_b^{\mathbf{B}_2} = \frac{\Phi}{\sqrt{2}}, \\ \mathbf{u}_c^{\mathbf{B}_3} &= \frac{\Phi}{\sqrt{2}}, \mathbf{e}_3 = \frac{\Phi}{\sqrt{2}}. \end{aligned} \quad (9)$$

Here  $m_0, A_0$  and  $\lambda_{4,0}$  are the values of the respective parameters at the scale  $\mu_0$  and  $D_1, D_2$  and  $D_3$  ( $|D_i| \ll 1 \forall i$ ) are the fine tuning parameters. Additionally in the field contents  $\mathbf{1} \leq \mathbf{B}_1, \mathbf{B}_2, \mathbf{B}_3 \leq \mathbf{3}$  are color indices,  $\mathbf{1} \leq \mathbf{a}, \mathbf{b}, \mathbf{c} \leq \mathbf{3}$  denote the indices for quark and lepton families and  $\mathbf{1} \leq \mathbf{I}_1, \mathbf{I}_2, \mathbf{I}_3, \mathbf{I}_4 \leq \mathbf{2}$  are the weak isospin indices. The flatness constraints require that  $\mathbf{B}_1 \neq \mathbf{B}_2 \neq \mathbf{B}_3$  for quarks,  $\mathbf{I}_1 \neq \mathbf{I}_2 \neq \mathbf{I}_3 \neq \mathbf{I}_4$ ,  $\sum_{\mathbf{d}=1}^3 \mathbf{P}_d^2 = \mathbf{1} \forall \mathbf{P}_d \in \mathbb{R}$  for leptons and  $\mathbf{a} \neq \mathbf{b} \neq \mathbf{c}$  for both. In eqn(8)  $m_\phi$  represents the soft SUSY breaking mass term,  $\phi$  the radial coordinate of the complex scalar field  $\Phi = \phi \exp(i\theta) (\in \mathbb{C})$  and the second term is the so called A-term which has a periodicity of  $2\pi$  in 2 D along

with an extra phase  $\theta_A$ . The radiative correction slightly affects the soft term and the value of the saddle point.

For  $n = 4$  we get an extremum for the principal values of  $\theta$  at  $\theta = \frac{(m\pi - \theta_A)}{4}$  (where  $\mathbf{m} \in \mathbb{Z}$ )

$$\begin{aligned} \phi_0 &= \sqrt{\frac{M}{4\lambda_4(3+D_3)}} \left[ A \left( 1 + \frac{D_2}{2} \right) \right. \\ &\quad \left. \pm \sqrt{A^2 \left( 1 + \frac{D_2}{2} \right)^2 - 8m_\phi^2(1+D_1)(3+D_3)} \right]^{\frac{1}{2}}, \end{aligned} \quad (10)$$

which appears from the constraint  $V'(\phi_0) = 0$  as a necessary condition for *saddle point*. However, this condition alone will not lead to *saddle point*. Rather, we have to make the potential sufficiently flat which can be achieved by vanishing higher derivatives of the potential. In this article, we consider non-vanishing fourth derivative of the potential resulting in saddle point. This will imply more fine-tuning but increased precision level in the information obtained from RG flow. Below we demonstrate how this is materialized.

As discussed,  $V''''(\phi_0) < 0$  will give us secondary local minimum. This leads to constraint relations:

$$A = \sqrt{2(3+D_3)G_1G_2G_3} m_\phi(\phi_0), \quad (11)$$

$$\begin{aligned} D_3 &= \frac{MA_0}{4\lambda_{4,0}\phi_0^2 \left( 37 + 60 \log \left( \frac{\phi_0}{\mu_0} \right) \right)} \left\{ D_2 \left( 13 + 12 \log \left( \frac{\phi_0}{\mu_0} \right) \right) \right. \\ &\quad \left. - \frac{2m_\phi^2(\phi_0)D_1M}{\lambda_{4,0}A_0\phi_0^2} + 6 \left( 1 - \frac{20\lambda_{4,0}\phi_0^2}{MA_0} \right) \right\}, \end{aligned} \quad (12)$$

one each for  $V''(\phi_0) = 0$  and  $V'''(\phi_0) = 0$ . In this context  $G_1 = \left[ \frac{(1+D_1)}{(3+D_3)}(15+11D_3) - (1+3D_1) \right]^2$ ,  $G_2 = \left[ (1+D_1)(3+\frac{7}{2}D_3) - (1+3D_1)(1+\frac{D_2}{2}) \right]^{-1}$ ,  $G_3 = \left[ \frac{(1+\frac{D_2}{2})}{(3+D_3)}(15+11D_3) - (3+\frac{7}{2}D_3) \right]^{-1}$ . For the limit  $|D_1| \ll 1, |D_2| \ll 1$  and  $|D_3| \ll 1$  which gives  $\phi_0 = \phi_0^{tree} \left[ 1 + \frac{D_1}{2} - \frac{D_3}{6} \right]^{\frac{1}{2}}$  and  $A \simeq A_{tree} \left[ 1 + \frac{D_1}{2} - \frac{D_3}{6} \right]$ , where  $\phi_0^{tree} = \sqrt{\frac{m_\phi(\phi_0)M}{\lambda_4\sqrt{6}}}$  and  $A_{tree} = 2\sqrt{6}m_\phi(\phi_0)$  represents tree level expressions. This means, during RG flow mentioning two parameters only ( $D_1$  and  $D_2$ ) will suffice instead of the usual three parameters in earlier MSSM models. This results in more precise information in RG flow. One may get tempted to vanish further higher derivatives of the potential in order to evaluate other unknown parameters ( $D_1$  and  $D_2$ ) without going into RG flow but this will make the effective inflaton potential in the vicinity of *saddle point* non-renormalizable. So, this is the highest level of precision constraint one can impose on RG flow parameters.

Consequently, around the *saddle point*  $\phi_0$ , the inflaton potential can be expanded in a Taylor series as,

$$V(\phi) = \tilde{C}_0 + \tilde{C}_4(\phi - \phi_0)^4, \quad (13)$$

where  $\tilde{C}_0 = V(\phi_0) = \frac{m_\phi^3(\phi_0)M}{6\sqrt{6}\lambda_4} \left\{ 3 \left( 1 + \frac{D_1}{2} - \frac{D_3}{6} \right) \left[ 1 + D_1 \log \left( \frac{\phi_0^2}{\mu_0^2} \right) \right] - 3 \left( 1 + \frac{D_1}{2} - \frac{D_3}{6} \right)^2 \left[ 1 + D_2 \log \left( \frac{\phi_0^2}{\mu_0^2} \right) \right] + \left( 1 + \frac{D_1}{2} - \frac{D_3}{6} \right)^2 \left[ 1 + D_2 \log \left( \frac{\phi_0^2}{\mu_0^2} \right) \right] \right\}$  and

$$\tilde{C}_4 = \frac{1}{4!} V''''(\phi_0) = \frac{m_\phi^2(\phi_0)}{24\sqrt{6}\phi_0^2} \left( 1 + \frac{D_1}{2} - \frac{D_3}{6} \right) \left\{ \left[ \left( \frac{360}{\sqrt{6}} - 12\sqrt{6} \right) + (684D_3 - 50\sqrt{6}D_2) \right] \left( 1 + \frac{D_1}{2} - \frac{D_3}{6} \right) - \frac{2\sqrt{6}D_1}{\left( 1 + \frac{D_1}{2} - \frac{D_3}{6} \right)} \right\} + \left( 1 + \frac{D_1}{2} - \frac{D_3}{6} \right) \left( \frac{360D_3}{\sqrt{6}} - 12\sqrt{6}D_2 \right) \log \left( \frac{\phi_0^2}{\mu_0^2} \right).$$

In what follows we shall model MSSM inflation with the above potential.

### III. MODELING MSSM INFLATION AND PARAMETER ESTIMATION

For brevity, let us introduce a change of parameter  $\phi \rightarrow x = \phi - \phi_0$  which represents the inflaton with shifted origin. Using this new notation of field the slow roll parameters [11] are given by,

$$\epsilon_v(x) = \frac{M^2}{2} \left( \frac{V'}{V} \right)^2 = \frac{8\tilde{C}_4^2 M^2 x^6}{(\tilde{C}_0 + \tilde{C}_4 x^4)^2}, \quad (14)$$

$$\eta_v(x) = M^2 \left( \frac{V''}{V} \right) = \frac{12\tilde{C}_4 M^2 x^2}{(\tilde{C}_0 + \tilde{C}_4 x^4)}, \quad (15)$$

$$\xi_v^2(x) = M^4 \left( \frac{V'V'''}{V^2} \right) = \frac{96\tilde{C}_4^2 M^4 x^4}{(\tilde{C}_0 + \tilde{C}_4 x^4)^2}, \quad (16)$$

$$\sigma_v^3(x) = M^6 \left( \frac{(V')^2 V''''}{V^3} \right) = \frac{384\tilde{C}_4^3 M^6 x^6}{(\tilde{C}_0 + \tilde{C}_4 x^4)^3}, \quad (17)$$

where a prime denotes  $d/d\phi = d/dx$ . During slow-roll inflation  $\epsilon_v, |\eta_v|, |\xi_v|, |\sigma_v| \ll 1$  and the end of the inflation corresponds to  $|x_f| \simeq \left( \frac{\tilde{C}_0^2}{8M^2\tilde{C}_4} \right)^{\frac{1}{6}}$  where  $x_f = \phi_f - \phi_0$ . In this context equation of state parameter can be expressed as

$$\omega(x) = \frac{P(x)}{\rho(x)} = \left[ \frac{-\tilde{C}_4^2 x^8 + \frac{16}{3}\tilde{C}_4^2 M^2 x^6 - 2\tilde{C}_0\tilde{C}_4 x^4 - \tilde{C}_0^2}{\tilde{C}_4^2 x^8 + \frac{16}{3}\tilde{C}_4^2 M^2 x^6 + 2\tilde{C}_0\tilde{C}_4 x^4 + \tilde{C}_0^2} \right] \quad (18)$$

which implies the energy scale of MSSM inflation is  $\tilde{C}_0^{\frac{1}{4}} \sim (0.409 - 1.301) \times 10^{-9}M$  explicitly shown in the allowed region in Fig(1).

The number of e-foldings are defined [11] for our model in the limit  $\tilde{C}_0 \gg \tilde{C}_4$  as

$$\mathcal{N} = \log \left( \frac{a(t_f)}{a(t_i)} \right) \simeq \frac{1}{M^2} \int_{x_f}^{x_i} \frac{V}{V'} dx \simeq \frac{\tilde{C}_0}{8M^2\tilde{C}_4} \left\{ \frac{1}{x_f^2} - \frac{1}{x_i^2} \right\}, \quad (19)$$

Further, in this framework the expressions for amplitude of the scalar perturbation, tensor perturbation and tensor to scalar ratio are given by

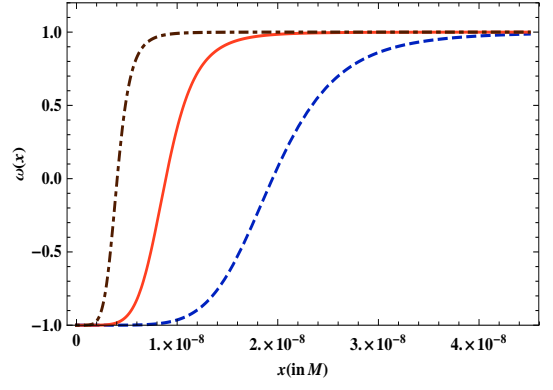


FIG. 1. Variation of equation of state parameter( $\omega(x)$ ) versus shifted inflaton field ( $x$ )

$$\Delta_s^2 = \frac{V^3}{75\pi^2 M^6 (V')^2} \Big|_{k=aH} = -\frac{32\tilde{C}_4 \mathcal{N}^3}{75\pi^2}, \quad (20)$$

$$\Delta_t^2 = \frac{V}{150\pi^2 M^4} \Big|_{k=aH} = \frac{(\tilde{C}_0 + \tilde{C}_4 x_*^4)}{150\pi^2 M^4}, \quad (21)$$

$$r = 16 \left( \frac{\Delta_t^2}{\Delta_s^2} \right) = -\frac{\tilde{C}_0}{4\tilde{C}_4 M^4 \mathcal{N}^3}. \quad (22)$$

Here  $x_*$  represents the value of the inflaton field at the horizon crossing. For our model expression for spectral index, running and running of the running reduces to the following form:

$$n_s - 1 = \frac{3\tilde{C}_0}{32\tilde{C}_4 M^4 \mathcal{N}^3} - \frac{3}{\mathcal{N}}, \quad (23)$$

$$n_t = \frac{\tilde{C}_0}{32\tilde{C}_4 M^4 \mathcal{N}^3}, \quad (24)$$

$$\alpha_s = \frac{3}{\mathcal{N}^2} - \frac{2}{3}(n_s - 1)^2, \quad (25)$$

$$\kappa_s = -\frac{6}{\mathcal{N}^3} - \frac{4}{\mathcal{N}^2}(n_s - 1) + \frac{8}{9}(n_s - 1)^3. \quad (26)$$

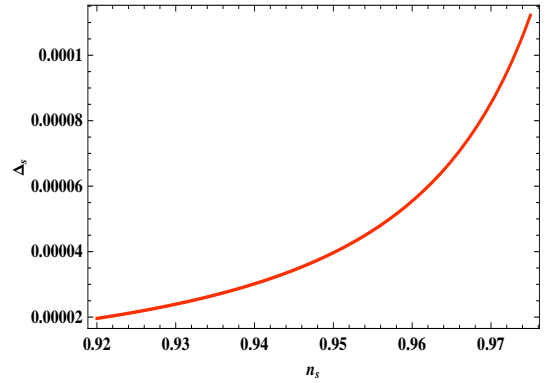


FIG. 2. Variation of the scalar power spectrum( $\Delta_s$ ) vs scalar spectral index( $n_s$ )

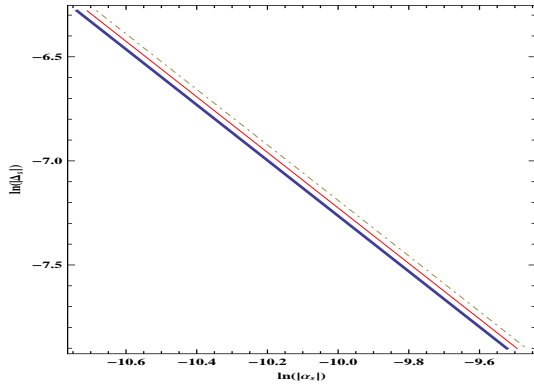


FIG. 3. Parametric plot of the logarithmic scaled amplitude of the scalar fluctuation ( $\ln(\Delta_s)$ ) vs logarithmic scaled amplitude of the running of the spectral index ( $\ln(|\alpha_s|)$ ) .

Fig(2) depicts the behavior of the scalar power spectrum as a function of scalar spectral index. For  $\mathcal{N} = 70$  the scalar spectral index is within the bounds of *WMAP7+BAO+h0 data* for model  $\Lambda$ CDM+*sz+lens* [8].

Fig(3) shows the behavior of amplitude of scalar fluctuation as a function of running of the spectral index. For the best fit value of  $\tilde{C}_0 = 2.867 \times 10^{-36} M^4$ ,  $\tilde{C}_4 = -1.685 \times 10^{-13}$  and  $\mathcal{N} = 70$  the cosmological parameters obtained from our model is  $\Delta_s^2 = 2.498 \times 10^{-9}$ ,  $\Delta_t^2 = 1.936 \times 10^{-39}$ ,  $n_s = 0.957$ ,  $n_t = -1.550 \times 10^{-30}$ ,  $r = 1.240 \times 10^{-29}$ ,  $\alpha_s = -0.612 \times 10^{-3}$ ,  $\kappa_s = 1.749 \times 10^{-5}$ .

Further, we use the publicly available code CAMB [12] to verify our results directly with observation. To operate CAMB at the pivot scale  $k_0 = 0.002 \text{ Mpc}^{-1}$  the values of the initial parameter space are taken for  $\tilde{C}_0 = 2.867 \times 10^{-36} M^4$  and  $\mathcal{N} = 70$ . Additionally WMAP7 years dataset [8] for  $\Lambda$ CDM background has been used in CAMB to obtain CMB angular power spectrum. In TableI we have given all the input parameters for CAMB. TableII shows the CAMB output, which is in good agreement with WMAP seven years data. In Fig.4 we have plotted CAMB output of CMB TT angular power spectrum  $C_l^{TT}$  for best fit with WMAP seven years data for scalar mode, which explicitly show the agreement of our model with WMAP7 dataset.

$H_0$ km/sec/MPc	$\tau_{Reion}$	$\Omega_b h^2$	$\Omega_c h^2$	$T_{CMB}$ K
71.0	0.09	0.0226	0.1120	2.725

TABLE I. Input parameters

$t_0$ Gyr	$z_{Reion}$	$\Omega_m$	$\Omega_\Lambda$	$\Omega_k$	$\eta_{Rec}$ Mpc	$\eta_0$ Mpc
13.707	10.704	0.2670	0.7330	0.0	285.10	14345.1

TABLE II. Output obtained from CAMB

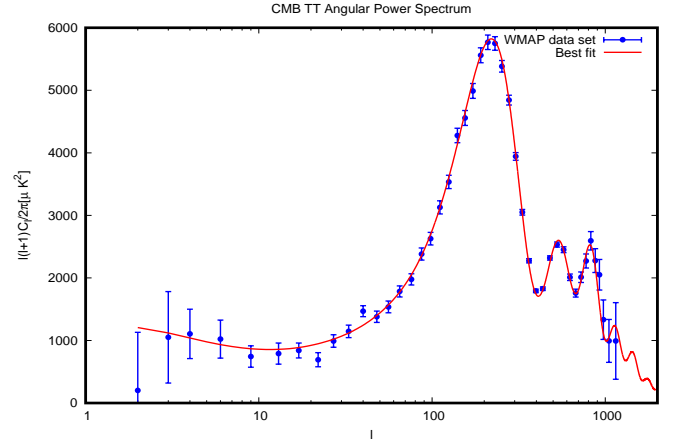


FIG. 4. Variation of CMB angular power spectrum  $C_l^{TT}$  for best fit and WMAP seven years data with the multipoles  $l$  for scalar mode

Now in the context of any running mass model one can expand the spectral index with the following parameterization [13]:

$$n_z(\mathcal{R}) = n_z(k_0) - \frac{\alpha_z(k_0)}{2!} \ln(k_0 \mathcal{R}) + \frac{\kappa_z(k_0)}{3!} \ln^2(k_0 \mathcal{R}) + \dots \quad (27)$$

with  $\mathcal{R} \ll 1/k_0$ , i.e.  $\ln(k_0 \mathcal{R}) < 0$ . This is identified to be the significant contribution to the Primordial Black Hole (PBH) formation. Here the parameterization index  $z : [s(\text{scalar}), t(\text{tensor})]$  and the explicit form of the first term in the above expansion is given by

$$n_z(k_0) = \begin{cases} n_s(k_0) - 1 & \text{if } z = s \\ n_t(k_0) & \text{if } z = t. \end{cases} \quad (28)$$

Existence of the running and running of the running is the key feature in the formation of PBH in the radiation dominated era just after inflation [14] which could form CDM in the Universe. The initial PBHs mass  $\mathcal{M}_{\text{PBH}}$  is related to the particle horizon mass  $\mathcal{M}$  by  $\mathcal{M}_{\text{PBH}} = \mathcal{M}\gamma = \frac{4\pi}{3}\gamma\rho\mathcal{H}^{-3}$  at horizon entry,  $\mathcal{R} = (a\mathcal{H})^{-1}$ . This is formed when the density fluctuation exceeds the threshold for PBH formation given as in *Press-Schechter theory* by [14, 15]

$$f(\geq \mathcal{M}) = 2\gamma \int_{\Theta_{\text{th}}}^{\infty} d\Theta \mathcal{P}(\Theta; \mathcal{M}(\mathcal{R})). \quad (29)$$

Here  $\mathcal{P}(\Theta; \mathcal{M}(\mathcal{R}))$  is the *Gaussian probability distribution function* of the linearized density field  $\Theta$  smoothed on a comoving scale  $\mathcal{R}$  by  $\mathcal{P}(\Theta; \mathcal{R}) = \frac{1}{\sqrt{2\pi}\Sigma_\Theta(\mathcal{R})} \exp\left(-\frac{\Theta^2}{2\Sigma_\Theta^2(\mathcal{R})}\right)$  where the standard deviation

$$\Sigma_\Theta(\mathcal{R}) = \sqrt{\int_0^\infty \frac{dk}{k} \exp(-k^2 \mathcal{R}^2) \Delta_\Theta^2(k)}. \quad (30)$$

For our model power spectrum for  $\Theta(k, \eta)$  is given by

$$\Delta_{\Theta}^2(k, \eta) = \frac{4J}{25} \left(\frac{k}{a\mathcal{H}}\right)^4 \Delta_s^2(k, \eta) = \frac{8J\sqrt{3\tilde{C}_0}Gk^4\eta^4(1+k^2\eta^2)}{25M\pi^2\kappa_s(\eta)}, \quad (31)$$

where  $\kappa_s(\eta) = \frac{18\sqrt{3}M^3G^3}{\tilde{C}_0^{\frac{3}{2}} \left[ \Phi(f) - MG\sqrt{\frac{3}{\tilde{C}_0}} \ln\left(\frac{\eta\alpha(t_f)\sqrt{\tilde{C}_0}}{\sqrt{3}M}\right) \right]^3}$  is the equivalent expression for running of the running in terms of conformal time  $\eta$  and  $J = \frac{(1+w)^2}{(1+\frac{3}{5}w)^2}$ . Additionally

we have used  $\Phi(f) = x_f^{-2}$  and  $G = \frac{8\tilde{C}_4M}{\sqrt{3\tilde{C}_0}}$ . Substituting eqn(31) in eqn(30) and using eqn(26) at the horizon crossing we get  $\Sigma_{\Theta}(\mathcal{R}) = \sqrt{\frac{8\sqrt{3}\tilde{C}_0JG}{25M\pi^2\kappa_s} \Gamma\left[\frac{n_s(\mathcal{R})+3}{2}\right]}$

for  $n_s(\mathcal{R}) > 3$ . Consequently eqn(29) gives  $f(\geq \mathcal{M}) = \gamma \text{erf}\left[\frac{\Theta_{\text{th}}}{\sqrt{2}\Sigma_{\Theta}(\mathcal{R})}\right]$ . Here we fix  $\gamma \simeq 0.2$  during the radiation dominated era [16] for proper numerical estimations. In general the mass of PBHs is expected to depend on the amplitude, size and shape of the perturbations [17]. As a consequence the PBH mass is given by [14]

$\mathcal{M}_{\text{PBH}} = \gamma \mathcal{M}_{\text{eq}}(k_{\text{eq}}\mathcal{R})^2 \left(\frac{g_{*,\text{eq}}}{g_*}\right)^{\frac{1}{3}}$ , where the subscript ‘‘eq’’ refers to the matter–radiation equality. Here we use  $g_* = 228.75$  (all degrees of freedom in MSSM), while  $g_{*,\text{eq}} = 3.36$  and  $k_{\text{eq}} = 0.07\Omega_m h^2 \text{ Mpc}^{-1}$  (Here we use  $\Omega_m h^2 = 0.2670$  from the CAMB output). Consequently the relation between comoving scale and the PBH mass in the context of MSSM is given by

$$\frac{\mathcal{R}}{1 \text{ Mpc}} = 1.250 \times 10^{-23} \left(\frac{\mathcal{M}_{\text{PBH}}}{1 \text{ g}}\right)^{\frac{1}{2}}. \quad (32)$$

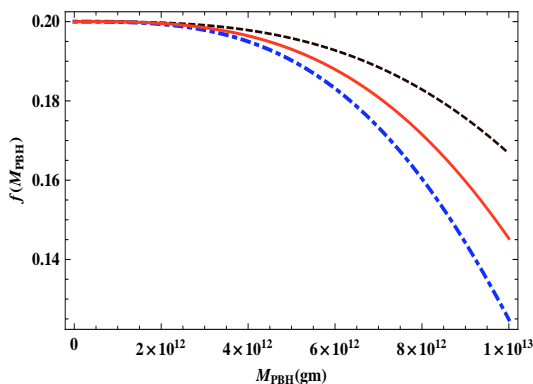


FIG. 5. Variation of the fraction of the energy density of the universe collapsing into PBHs as a function of the PBH mass, for three different values of the threshold  $\Theta_{\text{th}} = 0.3$ (dashed),  $0.5$ (solid),  $0.7$ (dotdashed).

Fig(5) shows the behavior of *Press–Schechter mass function* with respect to PBH mass. With the values of the parameters as obtained earlier, we have  $\mathcal{M}_{\text{PBH}} \simeq 10^{13} \text{ gm}$  and the corresponding fractional energy density  $f = 0.170$ .

Finally, the reheating temperature for our model turns out to be  $T_{rh} = \left(\frac{30x_*^2 M^2}{g_* \pi^2}\right)^{\frac{1}{4}} \sqrt{1200\pi^2 \tilde{C}_4^2 \Delta_s^2}$ . For  $\mathcal{N} = 70$  it is estimated as  $T_{rh} = 2.114 \times 10^8 \text{ GeV}$  which is obviously significant input to choose the fine tuned initial conditions for RGE flow discussed in the next section.

#### IV. ONE LOOP RG FLOW

For the flat direction **QQQL, QuQd, QuLe, uude** the soft SUSY breaking masses can be expressed as

$$\begin{aligned} (m_{\phi}^2)_{\text{QQQL}} &= \frac{1}{4}(m_{\tilde{Q}_a}^2 + m_{\tilde{Q}_b}^2 + m_{\tilde{Q}_c}^2 + m_{\tilde{L}_3}^2), \\ (m_{\phi}^2)_{\text{QuQd}} &= \frac{1}{4}(m_{\tilde{Q}_a}^2 + m_{\tilde{Q}_b}^2 + m_{\tilde{u}_c}^2 + m_{\tilde{d}_3}^2), \\ (m_{\phi}^2)_{\text{QuLe}} &= \frac{1}{4}(m_{\tilde{Q}_a}^2 + m_{\tilde{u}_b}^2 + m_{\tilde{L}_c}^2 + m_{\tilde{e}_3}^2), \\ (m_{\phi}^2)_{\text{uude}} &= \frac{1}{4}(m_{\tilde{u}_a}^2 + m_{\tilde{u}_b}^2 + m_{\tilde{d}_c}^2 + m_{\tilde{e}_3}^2), \end{aligned} \quad (33)$$

where  $1 \leq \mathbf{a}, \mathbf{b}, \mathbf{c} \leq 3$  and  $\mathbf{a} \neq \mathbf{b} \neq \mathbf{c}$ . After neglecting the contribution from the all Yukawa couplings except from the top we can express the one-loop beta function as [18]  $\beta_{m_a^2} = \dot{m}_a^2 = \frac{1}{8\pi^2} (m_a^2 + |A_U^{33}|^2) (\lambda_U^{33})^2 - \frac{1}{2\pi^2} \sum_{\alpha=1}^3 g_{\alpha}^2 |\tilde{m}_{\alpha}|^2 \mathbf{X}_{\alpha a}$  where  $\mathbf{X}_{\alpha a}$  are the quadratic Casimir Group Invariants for the superfield  $\Phi$ , defined in terms of Lie Algebra generators  $T^a$  by  $(T^{\alpha} T^{\alpha})_b^a = \mathbf{X}_{\alpha a} \delta_b^a$  and  $\dot{\mu} = \mu \frac{\partial}{\partial \mu}$ .

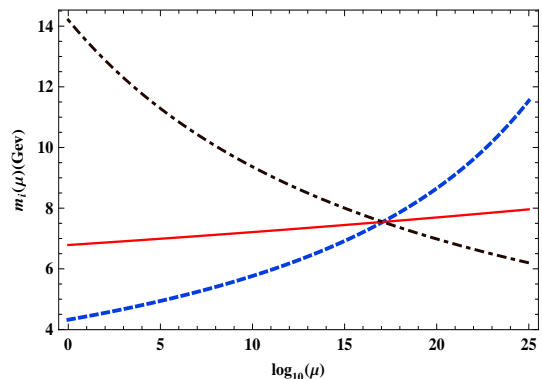


FIG. 6. Running of gaugino mass ( $m_i(\mu)$ ) in one loop RGE for MSSM with the logarithmic scale  $\log_{10}(\mu)$ . Here we have used  $\mu_0 = 2.6 \times 10^7 \text{ GeV}$ ,  $m_i(\mu_0) = 7.546 \times 10^{-3} \text{ TeV}$ ,  $\zeta = 1 \forall i$ .

In the context of MSSM  $\mathbf{X}_{1a} = \frac{3\mathbf{Y}_a^2}{5}$  (for each  $\Phi_a$  with weak hyper charge  $\mathbf{Y}_a$ ),  $\mathbf{X}_{2a} = \frac{3}{4}$  (for  $\Phi_a = \mathbf{Q}, \mathbf{L}, \mathbf{H}_u, \mathbf{H}_d$ ),  $= 0$  (for  $\Phi_a = \mathbf{\bar{u}}, \mathbf{\bar{d}}, \mathbf{\bar{e}}$ ),  $\mathbf{X}_{3a} = \frac{4}{3}$  (for  $\Phi_a = \mathbf{Q}, \mathbf{\bar{u}}, \mathbf{\bar{d}}$ ),  $= 0$  (for  $\Phi_a = \mathbf{L}, \mathbf{\bar{e}}, \mathbf{H}_u, \mathbf{H}_d$ ),

where  $\mathbf{X}_{1a}$ ,  $\mathbf{X}_{2a}$  and  $\mathbf{X}_{3a}$  are applicable for  $\mathbf{U}(1)_Y, \mathbf{SU}(2)_L$  and  $\mathbf{SU}(3)_C$  respectively. So for the flat direction content **QQQL, QuQd, QuLe, uude** we have the following beta functions:

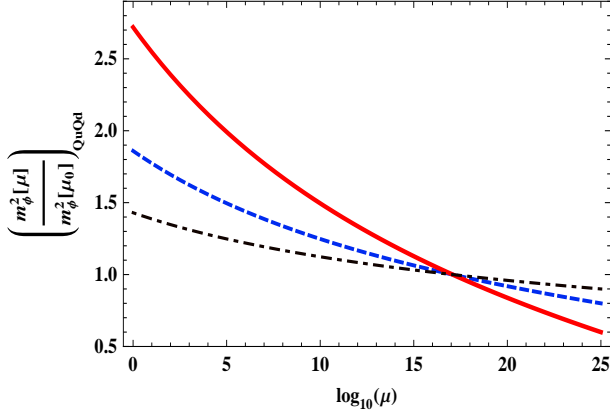


FIG. 7. Running of soft mass squared ratio  $\left(\frac{m_\phi^2(\mu)}{m_\phi^2(\mu_0)}\right)_{\text{QuQd}}$  in one loop RGE for MSSM with the logarithmic scale  $\log_{10}(\mu)$  where  $\mu_0 = 2.6 \times 10^7 \text{ GeV}$  for  $\zeta = 0.5, 1, 2$  for  $n = 4$  level **QuQd**  $\forall i$ . Similar plots can be obtained for **QuLe**, **QQQL** and **uude** flat directions also  $\forall i$ .

(a) **For Soft mass:**

$$\dot{\mu}(m_\phi^2)_{\text{QQQL}} = \frac{1}{8\pi^2} (3m_{Q_3}^2 + m_{U_3}^2 + |A_U^{33}|^2) (\lambda_U^{33})^2 - \frac{1}{8\pi^2} (3g_2^2 |\tilde{m}_2|^2 + 4g_3^2 |\tilde{m}_3|^2),$$

$$\dot{\mu}(m_\phi^2)_{\text{QuQd}} = \frac{1}{2\pi^2} (m_{Q_3}^2 + m_{U_3}^2) (\lambda_U^{33})^2 - \frac{1}{8\pi^2} \left( \frac{3}{2} g_2^2 |\tilde{m}_2|^2 + \frac{16}{3} g_3^2 |\tilde{m}_3|^2 \right),$$

$$\dot{\mu}(m_\phi^2)_{\text{QuLe}} = \frac{3}{8\pi^2} (m_{Q_3}^2 + m_{U_3}^2) (\lambda_U^{33})^2 - \frac{1}{8\pi^2} \left( \frac{3}{2} g_2^2 |\tilde{m}_2|^2 + \frac{8}{3} g_3^2 |\tilde{m}_3|^2 \right),$$

$$\dot{\mu}(m_\phi^2)_{\text{uude}} = \frac{1}{2\pi^2} (m_{Q_3}^2 + m_{U_3}^2) (\lambda_U^{33})^2 - \frac{1}{2\pi^2} g_3^2 |\tilde{m}_3|^2,$$

(b) **For Trilinear A-term:**

$$\dot{\mu}A_D^{aa} = \delta_{b3} (\lambda_U^{33})^2 \frac{A_U^{33}}{8\pi^2} - \frac{1}{4\pi^2} \left( \frac{7}{18} g_1^2 |\tilde{m}_1|^2 + \frac{3}{2} g_2^2 |\tilde{m}_2|^2 + \frac{8}{3} g_3^2 |\tilde{m}_3|^2 \right),$$

$$\dot{\mu}A_U^{ab} = \frac{3(1+\delta_{a3})A_U^{33}}{8\pi^2} (\lambda_U^{33})^2 - \frac{1}{4\pi^2} \left( \frac{13}{18} g_1^2 |\tilde{m}_1|^2 + \frac{3}{2} g_2^2 |\tilde{m}_2|^2 + \frac{8}{3} g_3^2 |\tilde{m}_3|^2 \right),$$

$$\dot{\mu}A_E^{aa} = -\frac{1}{4\pi^2} \left( \frac{3}{2} g_1^2 |\tilde{m}_1|^2 + \frac{3}{2} g_2^2 |\tilde{m}_2|^2 \right),$$

(c) **For Fourth level Yukawa coupling:**

$$\dot{\mu}\lambda_U^{aa} = \frac{3(1+\delta_{a3})}{8\pi^2} (\lambda_U^{33})^3 - \frac{\lambda_U^{aa}}{4\pi^2} \left( \frac{13}{18} g_1^2 + \frac{3}{2} g_2^2 + \frac{8}{3} g_3^2 \right),$$

$$\dot{\mu}\lambda_D^{ab} = \delta_{b3} (\lambda_U^{33})^2 \frac{\lambda_D^{ab}}{8\pi^2} - \frac{\lambda_D^{ab}}{4\pi^2} \left( \frac{7}{18} g_1^2 + \frac{3}{2} g_2^2 + \frac{8}{3} g_3^2 \right),$$

$$\dot{\mu}\lambda_E^{aa} = -\frac{\lambda_E^{aa}}{4\pi^2} \left( \frac{3}{2} g_2^2 + \frac{3}{2} g_3^2 \right)$$

where all the superscript a and b represent generation or family indices run from 1 to 3 physically representing the first, second and third generation respectively. For the one-loop renormalization of gauge couplings and gaugino masses, one has in general

$$\begin{aligned} \beta_{g_\alpha} &= \dot{\mu}g_\alpha = \frac{g_\alpha^3}{16\pi^2} [\Sigma_a \mathbf{I}_{\alpha a} - 3\mathbf{X}_{\alpha G}], \\ \beta_{m_\alpha} &= \dot{\mu}m_\alpha = \frac{g_\alpha^2 m_\alpha}{8\pi^2} [\Sigma_a \mathbf{I}_{\alpha a} - 3\mathbf{X}_{\alpha G}] \end{aligned} \quad (34)$$

where  $\mathbf{X}_{\alpha G}$  quadratic Casimir invariant of the group [ 0 for  $\mathbf{U}(1)$  and  $\mathbf{N}$  for  $\mathbf{SU}(\mathbf{N})$  ],  $\mathbf{I}_{\alpha a}$  is the Dynkin index of the chiral supermultiplet  $\Phi_a$  [ normalized to  $\frac{1}{2}$  for each fundamental representation of  $\mathbf{SU}(\mathbf{N})$  and to  $3\mathbf{Y}_a^2/5$  for  $\mathbf{U}(1)_Y$  ]. For the above mentioned flat direction the running of gauge couplings ( $g_i(\mu)$ ) and gaugino

masses ( $m_i(\mu)$ ) obey [18],  $\dot{\mu}g_i = \frac{d_i}{2}g_i^3$ ,  $\dot{\mu}\left(\frac{m_i}{g_i}\right) = 0 \forall i$  where for  $i = 1(\mathbf{U}(1)_Y), 2(\mathbf{SU}(2)_L), 3(\mathbf{SU}(3)_C)$  here  $d_1 = \frac{11}{8\pi^2}, d_2 = \frac{1}{8\pi^2}, d_3 = -\frac{3}{8\pi^2}$  which is the simpler version of the equation(34). Now to show explicitly that the contributions from the top Yukawa coupling ( $\lambda_U^{33}$ ) are very small for an induced electroweak group  $\mathbf{G}_{EW} = \mathbf{SU}(2)_L \otimes \mathbf{U}(1)_Y$  breakdown, let us start with the Higgs potential [18, 19]

$$\begin{aligned} V_{\text{Higgs}}(\mathbf{H}, \bar{\mathbf{H}}) &= m_1^2 |\mathbf{H}|^2 + m_2^2 |\bar{\mathbf{H}}|^2 + m_3^2 (\mathbf{H}\bar{\mathbf{H}} + \mathbf{H}^\dagger \bar{\mathbf{H}}^\dagger) \\ &\quad + \frac{1}{8} (g_1^2 + g_2^2) [|\mathbf{H}|^2 - |\bar{\mathbf{H}}|^2]^2, \end{aligned} \quad (35)$$

where  $\mathbf{H} = H_u$  and  $\bar{\mathbf{H}} = H_d$  represent the Higgs superfields and the relative vev of the two Higgses are given by

$$\begin{aligned} v &= \sqrt{\langle \mathbf{H} \rangle^2 + \langle \bar{\mathbf{H}} \rangle^2} \\ &= \sqrt{\frac{2[m_1^2 - m_2^2 - (m_1^2 + m_2^2) \cos(2\theta)]}{(g_1^2 + g_2^2) \cos(2\theta)}} \end{aligned} \quad (36)$$

with  $\tan(\theta) = \frac{\langle \bar{\mathbf{H}} \rangle}{\langle \mathbf{H} \rangle}$ . Here  $\theta$  represents an angular parameter which parameterizes MSSM. For the sake of convenience let us now write  $\cos(2\theta)$  appearing in equation(36) introducing new parameterization as [20]  $\cos(2\theta) = \frac{w^2 - 1}{w^2 + 1}$

where  $w = \frac{\langle \mathbf{H} \rangle}{\sqrt{1 - \left(\frac{\langle \bar{\mathbf{H}} \rangle}{\langle \mathbf{H} \rangle}\right)^2}}$ . Consequently the top Yukawa

coupling can be expressed as  $\lambda_U^{33} = \frac{m_U}{v \sin(\theta)}$  where  $0 \leq \theta < \frac{\pi}{2}$  and the top mass  $43 \text{ GeV} \leq m_U \leq 170 \text{ GeV} \ll \mu_{GUT}$  comes from the RG flow [18]. It is evident from the above parameterization [20–22] that as  $w \rightarrow 1$ ,  $\theta \rightarrow \frac{\pi}{4}$  which implies  $\langle \mathbf{H} \rangle$  and  $\langle \bar{\mathbf{H}} \rangle$  is very large and have the same order of magnitude. As a result the relative vev  $v$  is also large and the top Yukawa coupling is very very small for which one can easily neglect it from the RG flow at the energy scale of MSSM inflation as mentioned earlier. The consequence of the large vev of Higgs field can be taken care of by introducing strongly interacting gauge group  $\mathbf{G}_{\text{NEW}} = \mathbf{G}_8 \otimes \mathbf{SU}(3)_C$  and its superconformal version  $\mathbf{G}_{\text{SCONF}} = \mathbf{SU}(3)_{\text{SC}} \otimes \mathbf{SU}(3)_C$  [23].

In table(VI) we have tabulated the numerical values of vev of  $\mathbf{H}$  and  $\bar{\mathbf{H}}$ , the angular parameter  $\theta$ ,  $\tan(\theta)$ ,  $w$ , the top mass  $m_U$  and the top Yukawa coupling  $\lambda_U^{33}$  contributing to the parameter space of MSSM for the  $n = 4$  level flat directions **QQQL**, **QuQd**, **QuLe** and **uude**. It should be noted that appearance of large vev of Higgses as mentioned in table(VI) can easily be interpreted when Einstein Hilbert term appears in the total action of the theory at lowest order approximation [24] which is our present consideration. Consequently the contributions from the hard cutoff is sub-leading due to the soft conformal symmetry breaking. This leads to small top Yukawa coupling in the restricted parametric space of MSSM characterized by the phenomenological bound:  $43 \text{ GeV} \leq m_U \leq 170 \text{ GeV}$ ,  $1.006 \leq \tan(\beta) \leq 1.025$  for the  $n=4$  flat directions.

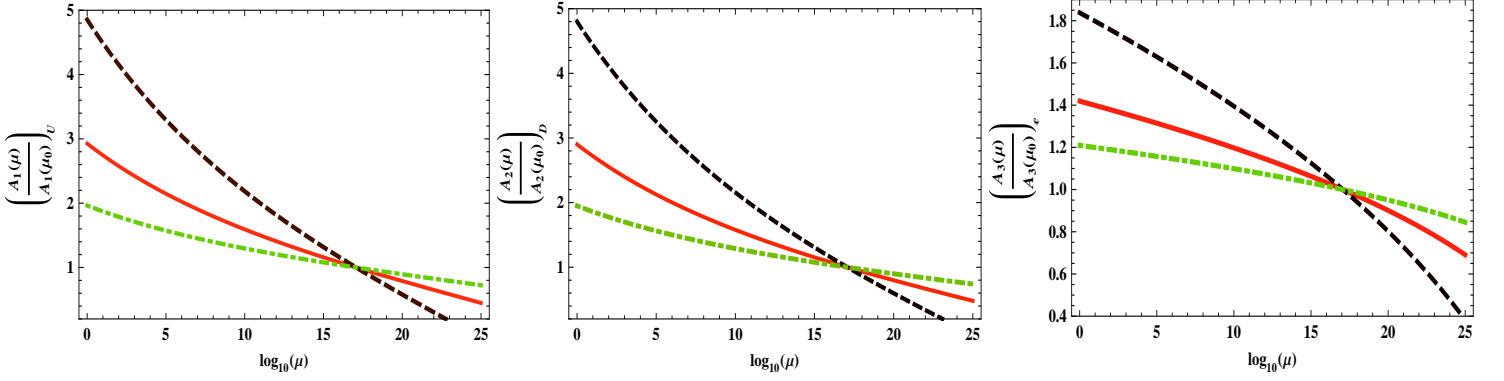


FIG. 8. Running of trilinear A -term ratio  $\left(\frac{A_\beta(\mu)}{A_\beta(\mu_0)}\right)_\nu$  in one loop RGE for MSSM with the logarithmic scale  $\log_{10}(\mu)$  where  $\mu_0 = 2.6 \times 10^7 GeV$ ,  $\zeta = 0.5$ (dotted-dashed), 1(solid), 2(dashed) and  $\beta = 1(U), 2(D), 3(E)$  for  $n = 4$  level  $\forall i$ .

Neglecting all the sub-leading contributions arising from the top Yukawa coupling in the restricted parameter space of the MSSM, the solutions of these RGE for  $n=4$  level flat directions can be written as

$$\begin{aligned}
 g_i(\mu) &= \frac{g_i(\mu_0)}{\sqrt{1-d_i g_i^2(\mu_0) \ln\left(\frac{\mu}{\mu_0}\right)}}, \\
 m_i(\mu) &= m_i(\mu_0) \left(\frac{g_i(\mu)}{g_i(\mu_0)}\right)^2, \\
 \Delta m_\phi^2 &= \sum_{i=1}^3 f_F^i \Delta m_i^2, \\
 \Delta A_\beta^{ab} &= \frac{1}{2} \sum_{i=1}^3 (C_\beta^i)^{ab} \Delta m_i, \\
 \lambda_\beta^{ab}(\mu) &= \lambda_\beta^{ab}(\mu_0) \prod_{i=1}^3 \left(\frac{g_i(\mu)}{g_i(\mu_0)}\right)^{(C_\beta^i)^{ab}},
 \end{aligned} \tag{37}$$

Here  $g_i(\mu_0)$ ,  $m_i(\mu_0)$ ,  $A_\beta(\mu_0)$ ,  $m_\phi(\mu_0)$  and  $\lambda_\beta(\mu_0)$  represent the value of the gauge couplings, gaugino masses, trilinear couplings, soft SUSY breaking masses and Yukawa couplings at the characteristic scale  $\mu_0$ . In equation(37) we have used the following shorthand notations:

$$\begin{aligned}
 \Delta A_\beta &= A_\beta(\mu) - A_\beta(\mu_0), \\
 \Delta m_i &= m_i(\mu) - m_i(\mu_0), \\
 \Delta m_\phi^2 &= m_\phi^2(\mu) - m_\phi^2(\mu_0), \\
 \Delta m_i^2 &= m_i^2(\mu) - m_i^2(\mu_0),
 \end{aligned}$$

where the  $\beta$  indices 1,2,3 represent U, D, E respectively.

$f_F^i$	$i = 1(\mathbf{U}(1)_Y)$	$i = 2(\mathbf{SU}(2)_L)$	$i = 3(\mathbf{SU}(3)_C)$
F=1(QQQL)	0	$\frac{3}{2}$	$-\frac{2}{3}$
F=2(QuQd)	0	$\frac{3}{4}$	$-\frac{8}{9}$
F=3(QuLe)	0	$\frac{3}{4}$	$-\frac{4}{9}$
F=4(uude)	0	0	$-\frac{2}{3}$

TABLE III. Entries of  $f_F^i$  matrix obtained from the solution of RGE

In equation (37)  $f_F^i$  and  $(C_\beta^i)^{ab}$  are  $(4 \times 3)$  and  $(3 \times 3)$  matrices whose entries are tabulated in Table(III) and Table(IV) respectively. It is obvious from the RGE that  $\beta = 1, 2$  implies  $a = b$  and  $\beta = 3$  implies  $a \neq b$ .

Using the solutions of RGE along with the approximation that the running of the gaugino masses and gauge

$(C_\beta^i)^{ab}$	$i = 1(\mathbf{U}(1)_Y)$	$i = 2(\mathbf{SU}(2)_L)$	$i = 3(\mathbf{SU}(3)_C)$
$\beta=1(\mathbf{U}), a=b$	$\frac{26}{99}$	6	$-\frac{32}{9}$
$\beta=2(\mathbf{D}), a=b$	$\frac{14}{99}$	6	$-\frac{32}{9}$
$\beta=3(\mathbf{E}), a \neq b$	$\frac{6}{11}$	6	0

TABLE IV. Entries of  $(C_\beta^i)^{ab}$  matrix obtained from the solution of RGE

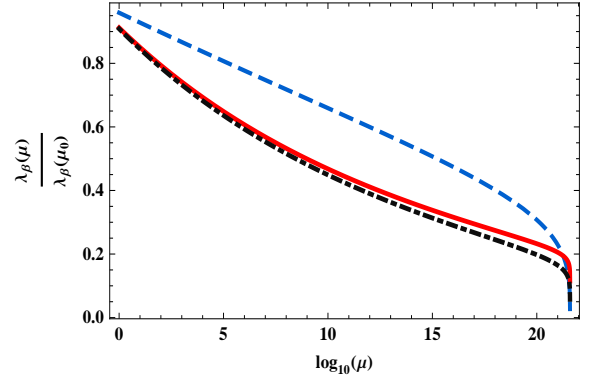


FIG. 9. Running of the ratio of the Yukawa coupling  $\left(\frac{\lambda_\beta(\mu)}{\lambda_\beta(\mu_0)}\right)$  in one loop RGE for MSSM with the logarithmic scale  $\log_{10}(\mu)$ . Here we have used  $\mu_0 = 2.6 \times 10^7 GeV$  and  $\beta = 1(U), 2(D), 3(E) \forall i$ .

couplings is very very small we get:

$$\begin{aligned}
 D_1 &= -\frac{1}{8\pi^2} \sum_{i=1}^3 J_i \left(\frac{m_i}{m_{\phi_0}}\right)^2 g_i^2(\mu_0), \\
 D_2^\beta &= -\frac{1}{4\pi^2} \sum_{i=1}^3 K^{\beta i} \left(\frac{m_i}{A_i}\right)^2 g_i^2(\mu_0),
 \end{aligned} \tag{38}$$

where we have  $J_1 = 0, J_2 = 3$  and  $J_3 = 4$  for  $i = 1, 2, 3$  and all the entries of  $K^{\beta i}$  ( $3 \times 3$ ) matrix are tabulated in table(V).

In this context the subscript '0' represents the values of parameters at the high scale  $\mu_0$ . As discussed in section III, constraining only  $D_1$  and  $D_2^\beta$

$K^{\beta i}$	$i = 1(\mathbf{U}(1)_Y)$	$i = 2(\mathbf{SU}(2)_L)$	$i = 3(\mathbf{SU}(3)_C)$
$\beta=1(\mathbf{U})$	$\frac{13}{18}$	$\frac{3}{2}$	$\frac{8}{3}$
$\beta=2(\mathbf{D})$	$\frac{7}{18}$	$\frac{3}{2}$	$\frac{8}{3}$
$\beta=3(\mathbf{E})$	$\frac{3}{2}$	$\frac{3}{2}$	0

TABLE V. Entries of  $K^{\beta i}$  matrix

is sufficient here. Eqn(12) provides an extra constraint relation which restricts the parameters further leading to more precise information in RG flow. For universal boundary conditions, the high scale is identified to be the GUT scale  $\mu_{GUT} \approx 3 \times 10^{16}$  GeV,  $\tilde{m}_1(\mu_{GUT}) = \tilde{m}_2(\mu_{GUT}) = \tilde{m}_3(\mu_{GUT}) = \tilde{m}$ ,  $A_E(\mu_{GUT}) = A_U(\mu_{GUT}) = A_D(\mu_{GUT}) = A_0$  and  $g_1 \approx 0.56$ ,  $g_2 \approx 0.72$ ,  $g_3 \approx 0.85$ . Now depending upon the different phenomenological situations the  $n = 4$  level flat directions are divided into two classes. The first class deals with **QuQd, QuLe** which is lifted completely at  $n = 4$  level. The other class which is lifted by higher dimensional operators deals with **uude, QQQL**. Most importantly **uude, QQQL** take part in the proton decay ( $p \rightarrow \pi^0 e^+$ ,  $p \rightarrow \pi^+ \nu_e$  etc.) [25] which introduces a stringent constraint on the Yukawa coupling  $\lambda_0$  at  $n = 4$  level. Additionally the neutrino-antineutrino oscillation data restricts  $\lambda_0$  again. Then we just use RG equations along with these restrictions to run the coupling constants and masses to the scales as mentioned in table(VI) with  $M = 2.4 \times 10^{18}$  GeV.

Considering all these values we obtain effectively

$$\begin{aligned}
D_1 &\approx -0.056\zeta^2, \\
D_2^1 &\approx -0.074\zeta, \\
D_2^2 &\approx -0.071\zeta, \\
D_3^1 &\approx -0.031\zeta, \\
D_3^2 &= D_3^3 = D_3^3 \approx -0.048 - 0.168\zeta^2,
\end{aligned}$$

where  $\zeta = m/m_\phi$  is calculated at the GUT scale. Typically the running based on gaugino loops alone results in negative values of  $D_i \forall i$ . Positive values can be obtained when one includes the Yukawa couplings, practically the top Yukawa, but the order of magnitude remains the same. The choice of fine tuned initial conditions directly shows more fine tuning is required compared to other models. It is a straightforward exercise to verify that even if one considers all the flat directions at  $n = 4$  level one will arrive at the potential eqn.(13) with same  $\tilde{C}_0$  and  $\tilde{C}_4$ . This is precisely what we have done in this paper.

The results of RG flow have been demonstrated in figs(6)-(9). In fig(6) and fig(7) ‘*dashed*’, ‘*solid*’ and ‘*dot-dashed*’ line represents  $\mathbf{U}(1)_Y$ ,  $\mathbf{SU}(2)_L$  and  $\mathbf{SU}(3)_C$  gauge group content respectively. Fig(6)-fig(9) explicitly showing the behavior of the RGE flow of gaugino masses, soft SUSY breaking mass, trilinear couplings and Yukawa couplings respectively. Additionally fig(6)-fig(8) give consistent GUT scale unification.

## V. SUMMARY AND OUTLOOK

In this article we have proposed a model of inflation in the framework of MSSM with new flat directions using saddle point mechanism. We have demonstrated how we can construct the effective inflationary potential in the vicinity of the *saddle point* starting from  $n = 4$  level superpotential for the flat direction content **QQQL, QuQd, QuLe** and **uude** for MSSM. The effective inflaton potential around saddle point, resulting from the non-vanishing fourth derivative of the original potential, has then been utilized in estimating for the observable parameters and confronting them with WMAP7 dataset using the publicly available code CAMB, which reveals consistency of our model with latest observations. We have then explored the possibility of Primordial Black Hole formation from the running-mass model by estimating the mass of PBH.

Subsequently, we have engaged ourselves in finding out the effective parameter space and the constants appearing in the *saddle point* analysis for the MSSM inflation by solving the one loop RGE. It is worth mentioning that the RGE flow of fourth level MSSM is exactly solvable in this context and we hope that all the numerics can be tested in the LHC or any linear collider in near future. Consequently we conclude that fourth level MSSM inflation confronts extremely well with WMAP7 within a certain parameter space obtained from one loop MSSM RGE flow.

A detailed survey of RG flow with two loop beta function, inflection point inflation [26] for  $n = 4$  level MSSM candidates, sensitivity in the neighborhood of the saddle point with the one loop corrected potential, the effect of quantum Coleman De Luccia tunneling [27] and the inflationary model building of MSSM derived from string theory via braneworld using several compactification schemes remain an open issue, which may even provide interesting signatures of MSSM inflation. We hope to address some of these issues in due course.

## ACKNOWLEDGMENTS

SC thanks H. P. Nilles, B. K. Pal and I. Singh for discussions and Council of Scientific and Industrial Research, India for financial support through Junior Research Fellowship (Grant No. 09/093(0132)/2010). SP is partially supported by the Alexander von Humboldt Foundation Germany, the SFB-Tansregio TR33 “The Dark Universe” (Deutsche Forschungsgemeinschaft) and the European Union 7th network program “Unification in the LHC era” (PITN-GA-2009-237920). We also acknowledge illuminating discussions with A. Mazumdar which helped in improvement of the article.

Flat direction	$\mu_0 = \phi_0$ GeV	$A_{0,tree}$ GeV	$m_{\phi_0}$ GeV	$\langle \mathbf{H} \rangle$ GeV	$\langle \bar{\mathbf{H}} \rangle$ GeV	$\theta$ in deg	$\tan(\theta)$	$w$	$v$ GeV	$m_U$ GeV	$\lambda_U^{33} = \lambda_0$ GeV
<b>QuLe</b>	$2.6 \times 10^7$	36.967	7.546	$0.200 \times 10^{16}$	$0.458 \times 10^{16}$	45.171	1.006	0.994	$0.500 \times 10^{16}$	43	$1.212 \times 10^{-14}$
<b>QuQd</b>	$2.6 \times 10^7$	36.967	7.546	$0.450 \times 10^{16}$	$0.423 \times 10^{16}$	45.370	1.013	0.987	$0.601 \times 10^{16}$	170	$7.106 \times 10^{-14}$
<b>QQQL</b>	$1.344 \times 10^{14}$	$892 \times 10^3$	$182 \times 10^3$	$0.188 \times 10^8$	$0.124 \times 10^8$	45.707	1.025	0.975	$0.226 \times 10^8$	80	$4.945 \times 10^{-6}$
<b>uude</b>	$2.896 \times 10^{13}$	$4.142 \times 10^6$	$845 \times 10^3$	$0.174 \times 10^6$	$0.157 \times 10^6$	45.549	1.019	0.981	$0.235 \times 10^6$	135	$8.047 \times 10^{-4}$

TABLE VI. MSSM parameter values obtained from RG flow for n=4 level flat directions

- 
- [1] A. Mazumdar and J. Rocher, Phys. Rept. 497 (2011) 85.  
[2] J. D. Barrow, R. Bean and J. Magueijo, MNRAS 316 (2000) L41.  
[3] R. Allahverdi, J. G. Bellido, K. Enqvist and A. Mazumdar, Phys. Rev. Lett. 97 (2006) 191304.  
[4] A. Chatterjee and A. Mazumdar, arXiv:1103.5758.  
[5] D. H. Lyth, JCAP 0704 (2007) 006; R. Allahverdi, K. Enqvist, J. G. Bellido, A. Jokinen and A. Mazumdar, JCAP 0706 (2007) 019.  
[6] K. Enqvist, A. Jokinen, S. Kasuya and A. Mazumdar, Phys. Rev. D 68 (2003) 103507.  
[7] CERN Large Hadron Collider, for more details see the online link: <http://public.web.cern.ch/public/en/lhc>.  
[8] WMAP collaboration, D. N. Spergel et al., Astrophys. J. Suppl. **170**, 377 (2007); for uptodate results on WMAP, see <http://lambda.gsfc.nasa.gov/product/map/current>.  
[9] Planck collaboration, <http://www.rssd.esa.int/index.php?project=Planck>, some early results are also available, see, for example, P. A. R. Ade et.al., arXiv:1101.2022.  
[10] T. Gherghetta, C. Kolda and S. P. Martin, Nucl. Phys. B 468 (1996) 37.  
[11] A. R. Liddle and D. H. Lyth, Cosmological Inflation and Large-Scale Structure, Cambridge University Press (2000).  
[12] CAMB, Online link: <http://camb.info/>  
[13] A. Kosowsky and M. S. Turner, Phys. Rev. D 52 (1995) 1739; N. Duechting, Phys. Rev. D 70 (2004) 064015.  
[14] M. Drees and E. Erfani, JCAP 1104 (2011) 005; M. Drees and E. Erfani, arXiv:1110.6052.  
[15] E. J. Copeland, A. R. Liddle, J. E. Lidsey and D. Wands, Phys. Rev. D 58 (1998) 063508.  
[16] B. J. Carr, Astrophys. J. 201 (1975) 1.  
[17] J. Niemeyer and K. Jedamzik, Phys. Rev. Lett. 80 (1998) 5481; J. Niemeyer and K. Jedamzik, Phys. Rev. D 59 (1999) 124013; M. Shibata and M. Sasaki, Phys. Rev. D 60 (1999) 084002; J. C. Hidalgo and A. G. Polnarev, Phys. Rev. D 79 (2009) 044006.  
[18] H. P. Nilles, Phys. Rept. (1984) 110.  
[19] S. P. Martin, hep-ph/9709356.  
[20] L. E. Ibanez and C. Lopez, CERN preprint TH-3650 (1983).  
[21] K. Inoue, A. Kakuto and S. Takeshita, Kyushu Univ. preprint 83 - HE - 6 (1983).  
[22] C. Kounnas, A. B. Lahanas, D. V. Nanopoulos and M. Quiros, CERN preprint TH - 3651 (1983).  
[23] T. Kobayashi, H. Nakano and H. Terao, Phys. Rev. D 71 (2005) 115009.  
[24] N. Kaloper, L. Sorbo and J. Yokoyama, Phys. Rev. D 78 (2008) 043527.  
[25] R. Harnik, D. T. Larson, H. Murayama and M. Thormeier, Nucl. Phys. B 706 (2005) 372.  
[26] S. Hotchkiss, A. Mazumdar and S. Nadathur, JCAP 1106 (2011) 002; K. Enqvist, A. Mazumdar and P. Stephens, arXiv:1004.3724; R. Allahverdi, B. Dutta and Y. Santoso, arXiv:1004.2741.  
[27] S. Coleman and F. De Luccia, Phys. Rev. D 21 (1980) 3305.